DOI 10.1515/ract-2013-2151 — Radiochim. Acta 2014; 102(5): 385–400

Jan Tits*, Xavier Gaona, Andreas Laube, and Erich Wieland

Influence of the redox state on the neptunium sorption under alkaline conditions: Batch sorption studies on titanium dioxide and calcium silicate hydrates

Abstract: Wet chemistry experiments were carried out to investigate the effect of the redox state and aqueous speciation on the uptake of neptunium by titanium dioxide (TiO_2) and by calcium silicate hydrates (C-S-H) under alkaline conditions. TiO_2 was chosen as a reference sorbent to determine the surface complexation behaviour of neptunium under alkaline conditions. C-S-H phases are important constituents of cement and concrete. They may contribute significantly to radionuclide retention due to their high recrystallization rates making incorporation the dominating sorption mechanism for many radionuclides (*e.g.* the actinides) on these materials. The sorption of neptunium on both solids was found to depend strongly on the degree of hydrolysis. On TiO_2 R_d values for Np(IV), Np(V) and Np(VI) are identical at pH = 10 and decrease with progressing hydrolysis in case of Np(V) and Np(VI). On C-S-H phases, R_d values for the three redox states are also identical at pH = 10. While the R_d values for Np(VI) sorption on C-S-H phases decrease with progressing hydrolysis, the R_d values for Np(IV) and Np(V) sorption are not affected by the pH. In addition to the effect of hydrolysis, the presence of Ca is found to promote Np(V) and Np(VI) sorption on TiO_2 whereas on C-S-H phases, the present wet chemistry data do not give unambiguous evidence. Thus, the aqueous speciation appears to have a similar influence on the sorption of the actinides on both types of solids despite the different sorption mechanism.

The similar R_d values for Np(IV,V,VI) sorption at pH = 10 can be explained qualitatively by invoking inter-ligand electrostatic repulsion between OH groups in the coordination sphere of Np(V) and Np(VI). This mechanism was proposed earlier in the literature for the prediction of actinide complexation constants with inorganic ligands. A limiting coordination number for each Np redox state, resulting from the inter-ligand electrostatic repulsion, allows the weaker sorption of the highest hydrolysed Np(V,VI) species to be explained.

Keywords: Neptunium, Redox, Sorption, Cement, C-S-H phases, TiO_2.

***Corresponding Author: Jan Tits,** Paul Scherrer Institut, Laboratory for Waste Management, CH-5232 Villigen PSI, Switzerland, e-mail: jan.tits@psi.ch

Andreas Laube, Erich Wieland: Paul Scherrer Institut, Laboratory for Waste Management, CH-5232 Villigen PSI, Switzerland

Xavier Gaona: Karlsruhe Institute of Technology, Institute for Nuclear Waste Disposal P.O. Box 3640, D-76021 Karlsruhe, Germany

1 Introduction

Cementitious materials are an important component in the multi-barrier concepts developed in many countries for the safe storage of low and intermediate level (L/ILW) radioactive waste in deep geological repositories (*e.g.*, [1]). Reliable thermodynamic models able to predict the interaction between radionuclides and cementitious materials in the long term are important for the performance assessment of future cement-based repositories. The development of such models requires a sufficiently detailed macroscopic and molecular-level understanding of the uptake processes involved. Studies on the retention of radionuclides by cementitious materials have focused predominantly on adsorption as the relevant uptake process (*e.g.*, [2] and references therein). However, other potentially important immobilization processes, such as incorporation in the solid matrix, may take place and, thus, exert a beneficial effect on radionuclide retardation. Calcium silicate hydrates (C-S-H), the major cement constituent, are characterized by high recrystallization rates (*e.g.*, [3]) thus making them an ideal system for the incorporation of radionuclides. Titanium dioxide (TiO_2) is a solid phase known to be stable under alkaline conditions and ambient temperature with low solubility and slow recrystallization [4]. Therefore, radionuclide incorporation into the

Brought to you by | Lib4RI Eawag-Empa
Authenticated
Download Date | 12/20/18 11:17 AM

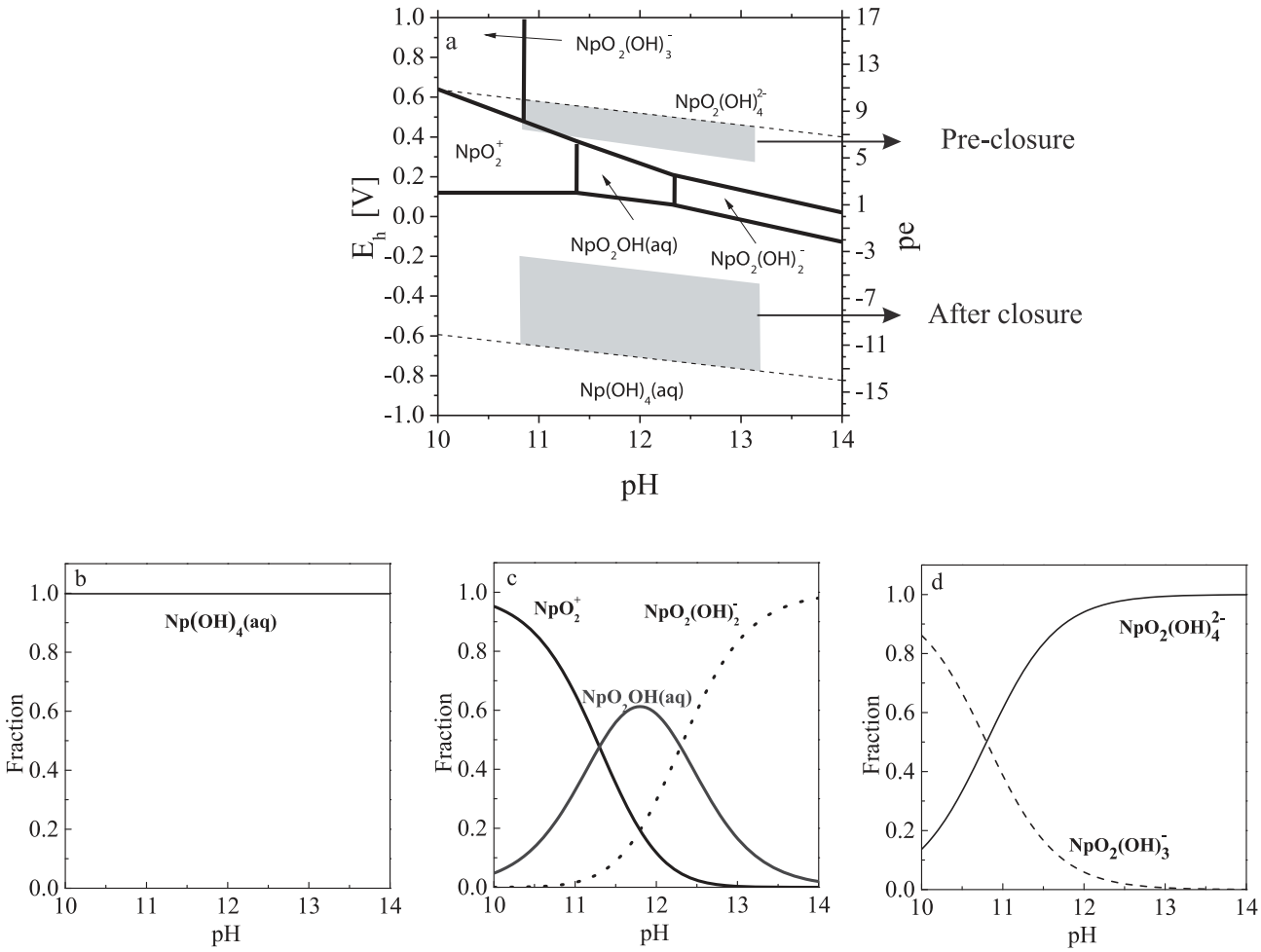

Fig. 1: Np predominance diagram (a) and Np(IV,V,VI) speciation (b, c, d) calculated using the NEA thermodynamic database [9] completed with stability constants for the hexavalent $NpO_2(OH)_2(aq)$ [5], $NpO_2(OH)_3^-$ and $NpO_2(OH)_4^{2-}$ species [10]. $I = 0$, $[Np]_{tot} = 10^{-10}$ M. The gray-coloured fields in the predominance diagram represent the redox potential ranges expected in the cementitious near-field of a L/ILW repository [11, 12].

structure of this mineral is unlikely, thus making it an adequate solid to study the surface complexation behaviour of radionuclides under alkaline conditions.

The chemical behaviour of neptunium in nuclear waste repositories is of particular concern because of its long half life ($t_{1/2} = 2.14 \times 10^6$ years) and its radiotoxicity. Neptunium is commonly believed to exist in the oxidation states +IV and +V in a cementitious environment under reducing and oxidizing conditions, respectively. However, the possible formation of anionic Np(VI) species ($NpO_2(OH)_3^-$ and $NpO_2(OH)_4^{2-}$) under oxidizing alkaline conditions, in analogy to U(VI), may significantly limit the stability field of Np(V) in favour of Np(VI) species. Recently, Np redox speciation studies have confirmed the analogy between the uranium and neptunium speciation under alkaline, oxidizing conditions [5]. A predominance diagramme for Np in the pH range $10 < pH < 14$ including the anionic Np(VI) species ($NpO_2(OH)_3^-$ and $NpO_2(OH)_4^{2-}$), shows that all three redox states may occur under the redox conditions expected in a L/ILW repository (gray-coloured regions in Figure 1a).

Experimental sorption data with Np(V) on cementitious materials are scarce while sorption data for Np(IV) and Np(VI) are non-existing in the literature due to the experimental difficulties associated with the stabilization of the +IV and +VI redox states (*e.g.*, [6]). Actinides are classified as hard Lewis acids and thus, they exhibit a strong affinity for oxygen-containing hard bases such as the surface hydroxyl groups of metal oxides and C-S-H phases (*e.g.*, [7]). These surface hydroxyl groups have oxygen atoms with lone electron pairs, which can act as electron donors in coordination reactions resulting in ionic bonding. The bond strength in ionic bonds correlates roughly with the effective charge of the metal cation [7, 8].

Brought to you by | Lib4RI Eawag-Empa
Authenticated
Download Date | 12/20/18 11:17 AM

Actinide surface complexation on C-S-H phases is thus expected to decrease with decreasing effective charge of the actinides in the order:

$$An^{4+}(4) > AnO_2^{2+}(3.3) > An^{3+}(3) > AnO_2^{+}(2.2) \quad (1)$$

Numbers in brackets represent the effective charge of the respective actinides [7, 8]. Studies with Th(IV) [13–18] report strong uptake behaviour with sorption distribution ratios (R_d values) typically $\geq 10^5$ L kg^{-1}. Th(IV) uptake by cementitious materials was interpreted in terms of inner-sphere complexation at the surface of the C-S-H phases in cement [16, 18]. Recently, an EXAFS study showed that C-S-H phases are responsible for Np(IV) retention by hardened cement paste (HCP) and that Np(IV) is predominantly incorporated in the interlayer of C-S-H phases [19].

A limited number of sorption data with Np(V) on HCP are available from the literature ([14, 20] and references herein) indicating strong sorption (R_d values ranging between 300 L kg^{-1} and 3×10^4 L kg^{-1}). This finding cannot be explained on the basis of the effective charge of NpO_2^+ and the ionic nature of the actinide surface complexes. EXAFS investigations carried out by Sylwester *et al.* [21] suggested that Np(V) is adsorbed on the cement surface in its pentavalent state in a first step, followed by reduction to the tetravalent state. The idea of a surface-catalysed reduction process is, however, not supported by a more recent XANES / EXAFS study [22]. The latter study shows the presence of pentavalent Np sorbed species on C-S-H phases and HCP after a reaction time of 2 months.

The same EXAFS study [22] also provided indications for incorporation of Np(VI) in the C-S-H interlayers based upon the presence of a neighbouring Si shell at short distance. Further information on the uptake of hexavalent actinides in C-S-H phases resulted from sorption studies with U(VI) on cementitious materials (*e.g.*, [22–28]). Measured R_d values were found to range between 10^3 L kg^{-1} and 10^6 L kg^{-1} and to depend on pH, aqueous speciation and the composition of C-S-H phases. The latter phases are considered to be responsible for U(VI) immobilization in cementitious materials. EXAFS investigations and luminescence spectroscopy studies further indicate that U(VI) is incorporated in the interlayer of the C-S-H phases [24, 27, 28]. Gaona *et al.* [29] finally showed that batch sorption data could be modelled with the help of a sublattice ideal solid solution model with three C-S-H end-members and three U(VI)-bearing end-members, in agreement with spectroscopic results.

The present study was carried out to determine a consistent set of sorption data for Np(IV), Np(V) and Np(VI) on C-S-H phases and on TiO_2 under alkaline conditions ($10 < pH < 14$) with the aim of 1) investigating the effect of the redox state of Np on the uptake by cementitious materials and 2) confirming the possibility of actinide incorporation in the C-S-H structure. Batch sorption experiments were carried out on C-S-H phases with varying composition and on TiO_2. The $CaO:SiO_2$ (C:S) mole ratios of C-S-H phases can vary between ~ 0.67 and ~ 2.0 (*e.g.*, [30]). With increasing C:S ratios, H^+ ions in the interlayer and bridging tetrahedra of the silica chains are progressively replaced by Ca^{2+} cations [31, 32]. The C:S ratio is known to correlate with both the pH and the aqueous Ca concentration (*e.g.*, [30, 33–35]). Hence, varying the C:S ratio in a sorption experiment coincides with a variation of pH and the aqueous Ca concentration. Sorption on TiO_2 was investigated to determine Np(IV,V,VI) surface complexation on oxide surfaces under alkaline conditions. Sorption experiments were carried out as a function of pH and aqueous Ca concentration to allow comparison with the sorption behaviour onto C-S-H phases to be made. Differences between the sorption behaviour on TiO_2 and on C-S-H phases were expected to provide evidence for incorporation into the C-S-H structure.

Control of the redox conditions during the batch sorption experiments was a critical aspect in this study. Reducing conditions were maintained by the addition of a reducing agent (Na-dithionite ($E_0(2SO_3^{2-}/S_2O_4^{2-}) = -1.13$ V), whereas oxidizing conditions were controlled by the addition of Na-hypochlorite (E_0 (Cl^-/ClO^-) = +0.8 V) as an oxidizing agent. The use of reducing or oxidizing agents, respectively, allowed redox conditions to be controlled at any time in the entire volume of the homogenized suspension.

To the best of our knowledge this paper reports the first measured R_d values for Np(IV) and Np(VI) on cementitious materials. These data will fill a major gap in sorption databases used in performance assessment studies for nuclear waste repositories.

2 Experimental

2.1 Materials

Throughout this study, Merck "Pro analysis" chemicals and deionized, decarbonated water (Milli-Q water) generated by a Milli-Q Gradient A10 System (Millipore, Bedford, USA) were used. The Milli-Q water was deaerated by purging thoroughly with N_2 for at least 2 h followed by equilibration with the inert N_2 glove box atmosphere for at least one week before use. The centrifuge tubes used for the wet chemistry experiments were washed, left overnight in a solution of 0.1 M HCl, and thoroughly rinsed with Milli-Q wa-

Brought to you by | Lib4RI Eawag-Empa
Authenticated
Download Date | 12/20/18 11:17 AM

ter. All experiments were carried out in glove boxes under N_2 atmosphere (pO_2, pCO_2 < 2 ppm).

Titanium dioxide (AEROXIDE P25) was obtained from Evonik Industries AG, Germany. This material is a mixture of 86% anatase and 14% rutile and has a specific surface area of 56 ± 1 m^2 g^{-1} [4, 36]. TiO_2 suspensions were prepared by mixing the appropriate amounts of Aeroxide P25 with 0.1 M NaCl solutions to obtain the solid to liquid (S:L) ratios required for the batch sorption tests. The pH of the suspensions was adjusted with NaOH solutions having concentrations of 0.01 M, 0.3 M and 1.0 M. The pH of the suspensions had to be adjusted several times over a period of 3 d to compensate for deprotonation reactions on the TiO_2 surface. TiO_2 suspensions with pH values above 13 were prepared in pure NaOH without 0.1 M NaCl as background electrolyte.

C-S-H phases with varying C:S ratios (0.65 < C:S < 1.65) were synthesised in Milli-Q water (alkali-free C-S-H phases) and in an artificial cement pore water (ACW) following a procedure adapted from [37]. Briefly, AEROSIL 300 (SiO_2) (Evonik Industries, AG, Germany) was mixed with CaO in polyethylene bottles to give target C:S ratios between 0.65 and 1.65. To this, ACW or Milli-Q water was added to achieve S:L ratios of 5×10^{-3} kg L^{-1}. After an ageing period of at least 2 weeks, the C-S-H suspensions were ready for further use in sorption experiments. A detailed characterization of these C-S-H phases is provided in [38]. The composition of ACW is based on an estimate of the pore water composition in HCP before any degradation of the material had occurred. The ACW contains 0.18 M KOH and 0.114 M NaOH and has a pH of 13.3. The Ca and Si concentrations of the pore water are fixed by the solubilities of the respective C-S-H phase. Part of the resulting suspensions (S : L = 5×10^{-3} kg L^{-1}) was centrifuged and the supernatant used to dilute the remaining suspension to the S:L ratio required for the batch sorption experiments.

^{239}Np tracer solutions were prepared according to a procedure described earlier by Sill [39]. The separation of this short-lived actinide isotope from its parent ^{243}Am (Eckert & Ziegler Isotope Products, USA) was achieved by extraction into long-chain amines (tri-iso-octylamine in xylene) followed by back-extraction with 0.01 M HCl.

^{45}Ca was used to determine Ca sorption and the aqueous Ca concentrations in TiO_2 suspensions. The ^{45}Ca stock solution was obtained from Imatom GmbH, Switzerland.

2.2 Methods

^{239}Np and ^{45}Ca activities in suspension and in solution were determined by liquid scintillation counting (LSC) using a Perkin Elmer Tri-Carb^{TM} A2750 CA liquid scintillation analyser with energy windows set between 4 and 330 keV and 4 and 125 keV, respectively. Prior to liquid scintillation analysis, 5 ml sample aliquots containing ^{239}Np or ^{45}Ca were mixed with 15 ml Ultima Gold XR scintillator (Perkin Elmer Inc., USA). Measured backgrounds were typically 50 ± 30 cpm/5 ml and 25 ± 10 cpm/5 ml, respectively, for the two tracers. Note that the C-S-H and TiO_2 concentrations in the suspensions were too low to cause significant quenching effects by the solid particles.

Solution compositions were determined using an Applied Research Laboratory ARL 3410D inductively coupled plasma optical emission spectrometer (ICP-OES). A combination glass pH electrode (Metrohm, Switzerland) calibrated against dilute standard pH buffers (pH = 7.0–11.0, Metrohm, Switzerland) was used to determine molar H^+ concentrations, $[H^+]$ (with $pH_c = -\log[H^+]$). In salt solutions of ionic strength $I \geq 0.1$ mol kg^{-1}, the measured pH value (pH_{exp}) is an operational apparent value related to $[H^+]$ by $pH_c = pH_{exp} + A_c$, where A_c is given as a function of NaCl and $CaCl_2$ concentrations [40]. In those systems with $[OH^-] > 0.1$ M, the H^+ concentration was calculated from the given OH^- concentration and the conditional ion product of water (pK'_w). Note that the actual $[H^+]$ can slightly deviate from calculated $[H^+]$ because a small amount of the added base is consumed in deprotonation reactions on the TiO_2 and C-S-H surfaces.

2.3 Experimental set-up

The uptake of the actinides by C-S-H phases and TiO_2 was studied by determining their partitioning between solid and liquid phase. The uptake was expressed in terms of a distribution ratio, R_d (L kg^{-1}), which is the ratio of the amount of radionuclide sorbed, $\{M_{sorb}\}$ (mol kg^{-1}) and the radionuclide concentration in solution, $[M]_{eq}$ (M). The R_d value was obtained from activity measurements in suspensions and in supernatant solutions using the following equation:

$$R_d = \frac{\{M\}_{sorb}}{[M]_{eq}} = \frac{[M]_{sorb}}{[M]_{eq}} \cdot \frac{V}{m} = \frac{\left(A_{susp} - A_{eq}\right)}{A_{eq}} \cdot \frac{V}{m} \quad \text{L kg}^{-1} \tag{2}$$

where $[M]_{sorb}$ is the concentration of radionuclide sorbed on the solid (M). A_{susp} is the activity determined in suspension (Bq L^{-1}), A_{eq} is the activity determined in the supernatant solution (Bq L^{-1}), V is the sample volume (L) and m is the mass of C-S-H phase and TiO_2 in suspension (kg).

Brought to you by | Lib4RI Eawag-Empa
Authenticated
Download Date | 12/20/18 11:17 AM

Table 1: List of sorption experiments and experimental conditions

Sorbent	Rn	Experiment	Np Redox state	Eq. time (d)	pH_c	Initial [Ca]
TiO_2	^{45}Ca	Isotherm		3	12.2	1.3×10^{-6}–2.5×10^{-3} M
					13.23	1.3×10^{-6}–1.0×10^{-3} M
					13.77	1.3×10^{-6}–4.0×10^{-4} M
	^{239}Np	pH dependence	IV, V, VI	3	10.0–14.2	0
		Dependence on [Ca]	IV, V, VI	3	12.0	0–2.5×10^{-3} M
				3	13.3	0–1.6×10^{-3} M
C-S-H phases	^{239}Np	Kinetics	V	1–120	10.1	4.8×10^{-4} M[a]
					12.0	5.8×10^{-3} M[a]
					12.4	2.0×10^{-2} M[a]
		Dependence on C-S-H composition	IV, V, VI	3	10.1–12.5 (alkali-free)	4×10^{-4}–2.0×10^{-2} M[a]
					13.3 (ACW)	4.0×10^{-5}–1.6×10^{-3} M[a]

[a] Equilibrium [Ca].

Batch-type sorption tests with ^{239}Np were carried out as a function of the equilibration time (sorption kinetic tests) and as a function of the solid composition (C:S ratio) in systems with C-S-H phases, and as a function of pH and aqueous Ca concentration in systems with TiO_2. An overview of all the experiments performed in the frame of this investigation is given in Table 1. Note that sorption kinetic tests were actually only carried out with Np(V) on C-S-H phases. The sorption kinetics of Np(IV,V,VI) on TiO_2 were not measured because there is ample evidence in the literature for the fast sorption of tetravalent, pentavalent and hexavalent actinides onto TiO_2 and other metal oxides (see section 3.1. for further details). TiO_2 suspensions with a S:L ratio of 2.0×10^{-4} kg L^{-1} and C-S-H suspensions with a S:L ratio of 5.0×10^{-4} kg L^{-1} were prepared in 40 mL centrifuge tubes as described above. To these suspensions, aliquots of ^{239}Np radionuclide solutions were added. The total concentration of ^{239}Np in the sorption tests was 1.5×10^{-10} M. The redox state of neptunium was controlled by addition of 5×10^{-3} M Na-dithionite ($Na_2S_2O_4$) or 10^{-2} M Na-hypochlorite (NaClO), respectively. Gaona *et al.* [19, 22] and Rojo *et al.* [41] showed that Na-dithionite and Na-hypochlorite have no influence on the sorption behaviour of tetravalent and hexavalent actinides. XANES spectra of C-S-H pastes containing much higher ^{237}Np concentrations ($> 10^{-5}$ M) in the pH range, $9 < pH < 13.5$ confirmed that these reducing/oxidizing agents were able to keep Np in the tetravalent and the hexavalent states, respectively [19, 22]. In addition, the sorption behaviour of Np(IV) and Np(VI) on C-S-H phases observed in the present experiments (see section 3.3) is similar to the sorption behaviour of Th(IV) and U(VI) onto C-S-H phases reported in the literature [27, 41]. *i.e.*, the R_d values for Np(IV) and Th(IV) sorption on C-S-H phases are both independent of the C:S ratio whereas R_d values for Np(VI) and the U(VI) sorption both decrease with increasing C:S ratio. The absolute R_d values for both actinides are not identical but the trends are similar. Thus, it may be safely assumed that Na-dithionite and Na-hypochlorite are capable of controlling the redox state of ^{239}Np at the much lower concentrations used in the present experiments.

Ca sorption isotherms on TiO_2 were determined as follows: Increasing volumes of a 5×10^{-3} M $CaCl_2$ solution labelled with ^{45}Ca were added to TiO_2 suspensions (S:L = 10^{-3} kg L^{-1}) prepared in NaOH solutions at three different concentrations: 0.02 M, 0.3 M and 1.0 M to achieve total Ca concentrations varying between 2.5×10^{-3} M and 1.3×10^{-6} M.

The centrifuge tubes containing the ^{45}Ca or ^{239}Np labelled TiO_2 and C-S-H suspensions were equilibrated on an end-over-end shaker. After regular time intervals (kinetic tests) or after three days (other experiments), the suspensions were sampled, and the samples were stored for further analysis.

Phase separation of the remaining suspensions was carried out by centrifugation (1 h at 90 000 g (max)) followed by sampling of the supernatant solutions. Samples before centrifugation were taken in duplicate, samples after centrifugation in triplicate. ^{239}Np activities in the suspensions and in the supernatant were determined together with standards and blanks by LSC as described above.

The sorption samples with ^{239}Np were equilibrated for only three days, because the short ^{239}Np half-life (2.355 d) and the low activities remaining in the supernatant after sorption in many experiments did not enable longer equilibration times. Sorption kinetics tests (section 3.1) showed that such short equilibration times may result in an underestimation of the R_d value of 30% at maximum. In order to account for possible underestimations and for other uncertainties on the sorption measurements, the relative

Brought to you by | Lib4RI Eawag-Empa
Authenticated
Download Date | 12/20/18 11:17 AM

uncertainties on all the R_d values presented in this study were set to 60%.

3 Results

3.1 Kinetic test experiments

The sorption kinetic was determined for Np(V) on C-S-H phases under alkali-free conditions (Figure 2). For all C-S-H phases, equilibrium was found to be attained within 8 days. Uptake by C-S-H phases with lower C:S ratio appears to be slightly slower (equilibrium after 8 days) than uptake by C-S-H phases with a C:S ratio of 1.65 (1–2 d). Fast uptake could indicate a surface complexation process whereas the slower uptake observed in the C-S-H systems with low C:S ratios suggest that other processes with slower kinetics, such as diffusion into the C-S-H interlayers or recrystallization, could be important.

Sorption kinetics with Np(IV) and Np(VI) on C-S-H phases were not determined. Previous kinetic studies with Th(IV) and U(VI), however, showed that uptake of tetravalent and hexavalent actinides by C-S-H phases occurs within time scales similar to those of Np(V). In the case of Th(IV), maximum R_d values were determined after less than 1 day, whereas in the case of U(VI) maximum sorption was observed after approximately 10 d [27, 42].

The sorption of Np(IV), Np(V) and Np(VI) on TiO_2 was assumed to be fast based upon previous investigations with Th(IV), Np(V) and U(VI). Guo *et al.* [43, 44] showed that the kinetics of U(VI) and Th(IV) on TiO_2 are very fast over a wide pH range, with maximum sorption being reached within 1 day. Furthermore, studies on iron oxides and clays indicate fast Np(V) sorption kinetics (*e.g.*, [45–48]) supporting the assumption that the sorption kinetics of Np(V) on TiO_2 is fast.

In conclusion, the present sorption kinetic tests along with literature data indicate that Np(IV,V,VI) uptake is very fast, reaching maximum sorption within 1–2 d if surface compexation dominates (*e.g.* on TiO_2). The slightly slower sorption kinetics on C-S-H phases (sorption equilibrium within 8 d) suggest, however, that additional uptake processes such as diffusion into the C-S-H interlayers or recrystallization, might occur.

3.2 Sorption studies on TiO_2

The results from batch sorption tests with Np(IV,V,VI) onto TiO_2 are shown as function of pH (Figure 3) and as function of the aqueous Ca concentration (Figure 4). Note that

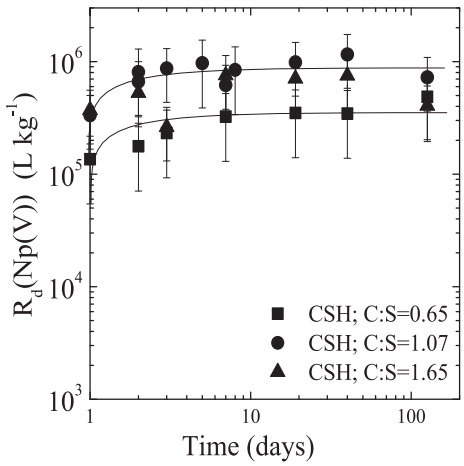

Fig. 2: Kinetics of the Np(V) sorption onto C–S–H phases with different C:S ratios under alkali-free conditions.

due to the extremely low ^{239}Np concentrations used in the present experiments ($[^{239}Np]_{tot} = 1.6 \times 10^{-10}$ M), the formation of aqueous polynuclear species or solid phases can be excluded.

3.2.1 Sorption of Np(IV,V,VI) species at high pH

At pH = 10.1, Np(IV,V,VI) were found to sorb strongly on TiO_2 (R_d values ranging from 5×10^5 L kg^{-1} to 3×10^6 L kg^{-1}). Such high R_d values are expected for Np(IV) and Np(VI) due to their effective charge of 4.0 and 3.3, respectively, and the claimed correlation between ionic bond strength and effective charge (1). Furthermore, high R_d values are in agreement with the sorption values determined for Th(IV) and U(VI) on various solids under alkaline conditions in the absence of CO_2 (*e.g.*, [49–51]). The strong sorption of Np(V) was not anticipated as the low effective charge (2.2, NpO_2^+) rather suggests weak to moderate sorption. Np(V) sorption data reported for various types of solids at pH = 10 are controversial. Measured R_d values were found to vary from 1.0–400 L kg^{-1} on quartz [45, 46, 52], 4×10^2–3×10^4 L kg^{-1} on clay minerals [45, 47, 53, 54] and 8×10^3–10^5 L kg^{-1} on Fe-oxides [52, 55]. This variation in R_d values could be explained partially by sorbent properties such as the effect of surface loading (non-linear sorption) and sorption capacity of the different solids [45]. Furthermore, the type of Np(V) surface complexes formed (monodentate–multidentate) could influence measured R_d values as well. With a view to the other high R_d values determined with Np(V) on oxides at pH = 10 [52, 55], the high R_d values determined for Np(V) sorption on TiO_2 are not exceptional. Taking into account the correlation between ionic bond

Brought to you by | Lib4RI Eawag-Empa
Authenticated
Download Date | 12/20/18 11:17 AM

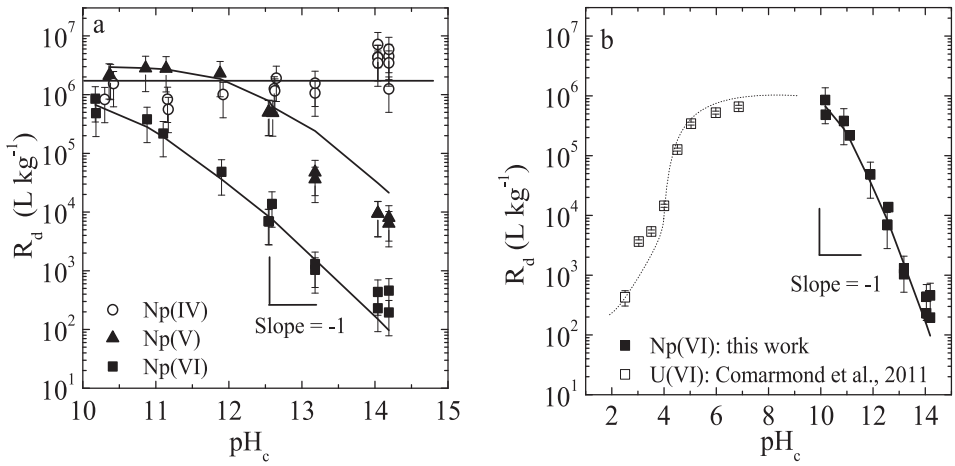

Fig. 3: Sorption of Np(IV,V,VI) on TiO_2 under alkaline conditions. a) Effect of pH. b) Comparison of Np(VI) sorption under alkaline conditions with U(VI) sorption at low and neutral pH (Comarmond *et al.* [36] and Comarmond, pers. comm.). The solid lines are shown to guide the eye.

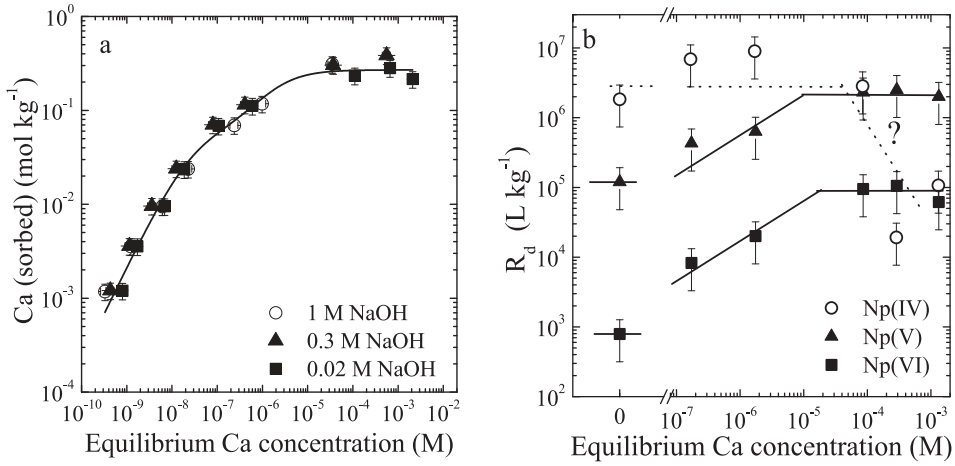

Fig. 4: Effect of the Ca concentration on Np(IV,V,VI) sorption on TiO_2. a) Ca sorption isotherms at three different NaOH concentrations. b) Np(IV,V,VI) sorption as function of the equilibrium Ca concentration in ACW (pH = 13.3). The solid lines are shown to guide the eye.

strength and effective charge (1), the R_d values for Np(IV) and Np(VI) should then be much higher compared to the R_d values for Np(V), which is not the case.

3.2.2 Effect of the pH

In the case of Np(IV), the pH had no influence on its sorption behaviour (Figure 3a). Aqueous speciation under alkaline conditions shows that the neutral $Np(OH)_4(aq)$ species is the only species present above pH = 10 (Figure 1b.), and therefore Np(IV) sorption onto TiO_2 does not depend on pH.

Figure 3a further reveals that Np(V,VI) uptake by TiO_2 decreases with increasing pH. In the case of Np(V), this behaviour is attributed to variations in the aqueous speciation over the pH range under investigation. Indeed, speciation calculations for Np(V) in the range $10 < pH < 14$ (Figure 1c) reveal that the observed drop of the R_d value above pH = 12 corresponds very well with the increasing dominance of the anionic $NpO_2(OH)_2^-$ species in solution. This indicates that the affinity of this anionic species for the negatively charged TiO_2 surface is very low.

Combination of the Np(VI) sorption data and the U(VI) sorption data determined by Comarmond *et al.* [36] on the same Aeroxide P25 TiO_2 suggests that the R_d value for the sorption of hexavalent actinyl ions reaches a maximum ($\sim 10^6$ L kg^{-1}) in the pH range $7 < pH < 10$ (Figure 3b). This maximum R_d value coincides with the predominance of the anionic $NpO_2(OH)_3^-$ or $UO_2(OH)_3^-$ species, respectively (see Figure 1d). The observed drop of the R_d value above pH = 10 corresponds very well with the increasing predominance of the anionic $NpO_2(OH)_4^{2-}$ species in solution. These observations indicate that, notwithstanding

Brought to you by | Lib4RI Eawag-Empa
Authenticated
Download Date | 12/20/18 11:17 AM

its negative charge, the anionic species, $NpO_2(OH)_3^-$, is strongly sorbing on the TiO_2 surface. Hence, electrostatic repulsion does not prevent anionic Np-hydroxy species from sorbing on negatively charged TiO_2 surface sites.

3.2.3 Effect of Ca

Sorption experiments with Ca on TiO_2 at different NaOH concentrations (0.02 M, 0.3 M and 1.0 M) showed very strong sorption under alkaline conditions. At the lowest loading the R_d value was determined to be ~ 5×10^6 L kg^{-1}. Note that the high R_d value observed for Ca (effective charge = 2), is in agreement with the high R_d values determined for Np(V) (effective charge = 2.2). The Ca isotherms measured at different NaOH concentrations are identical and exhibit a non-linear shape (Figure 4a). The Ca loading reaches a maximum of ~ 0.3 mol kg^{-1} at an aqueous Ca concentration of ~ 10^{-5} M. Assuming a site density in the range between 2 to 12 sites per nm^2 [56, 57] and a specific surface area of 56.9 m^2 g^{-1} [36], this means that virtually all TiO_2 sorption sites are occupied by Ca at maximum loading. Strong Ca sorption onto TiO_2 is in agreement with earlier studies on Ca sorption on TiO_2 under neutral to slightly alkaline conditions (see *e.g.*, [58–61]).

The effect of the aqueous Ca concentration on the Np(IV,V,VI) uptake by TiO_2 in ACW at pH = 13.3 is shown in Figure 4b. The sorption data reveal that R_d values for Np(IV) are independent of the Ca concentration up to a Ca concentration of 10^{-4} M. Above this concentration, however, R_d values appear to decrease. A similar experiment carried out at pH = 12 however, did not confirm this decrease of the R_d values (data not shown). At present, we have no conclusive explanation for this behaviour.

Np(V,VI) sorption onto TiO_2 in ACW (pH = 13.3) was found to increase with increasing aqueous Ca concentration up to an equilibrium Ca concentration of ~ 10^{-5} M. The latter Ca concentration corresponds to maximum site saturation on TiO_2. Above this concentration, the sorbing Np thus binds to a "Ca-OH" like surface rather than to a "Ti-OH" like surface. Similar trends were observed at pH = 12 and at pH = 14. (data not shown): At pH = 12, an increase in equilibrium Ca concentration from 0 to ~ 10^{-4} M did not affect neither the Np(IV) sorption nor the Np(V) sorption, but increased the R_d value for Np(VI) sorption from ~ 2×10^4 L kg^{-1} to ~ 2×10^6 L kg^{-1}. At pH = 14, an increase in the equilibrium Ca concentration from 0 to ~ 10^{-5} M had no effect on the Np(IV) sorption but increased the R_d value for Np(V) from ~ 10^4 L kg^{-1} to ~ 10^6 L kg^{-1} and the R_d value for Np(VI) from ~ 10^2 L kg^{-1} to ~ 10^6 L kg^{-1}.

The effect of Ca sorption on Np(V,VI) sorption can be explained either by neutralisation of the negative surface charge, or by the formation of a very strong surface-stabilized Ca-neptunate complex or Ca–neptunate ion pair. A thorough understanding of the Np(V,VI) sorption processes on TiO_2 under alkaline conditions in the presence of Ca would require a more in-depth wet-chemistry and spectroscopic investigation exceeding the scope of the present study.

Thus, we only conclude that Ca sorption significantly increases Np(V) and Np(VI) uptake by TiO_2.

3.3 Sorption studies on C-S-H phases

The uptake of Np(IV,V,VI) by C-S-H phases was determined as function of the C:S ratio under alkali-free conditions (Figure 5a) and in the presence of alkalis, *i.e.* ACW at pH = 13.3 (Figure 5b, c). The C:S ratio of C-S-H phases correlates with both the pH and the Ca concentration in solution (*e.g.*, [30, 33–35, 38]). An increase in the C:S ratio from 0.67 to 1.65 results in a pH increase from 10.1 to 12.5 and an increase in the Ca concentration from ~5×10^{-4} M to 2×10^{-2} M. In ACW, at a constant pH of 13.3, the Ca concentration increases from ~ 10^{-5} M to 1.6×10^{-3} M at increasing C:S ratios between 0.67 and 1.29 [38]. The change in the C:S ratio further induces changes in the structure of the C-S-H phases. To test how much of the Np(IV,V,VI) sorption behaviour can be explained by their speciation in solution, the Np(IV,V,VI) sorption behaviour on C-S-H phases was interpreted in terms of pH and aqueous Ca concentration in agreement with the sorption behaviour on TiO_2.

R_d values determined for Np(IV) on C-S-H phases under alkali-free conditions were found to be very high ($(6 \pm 3) \times 10^5$ L kg^{-1}) and appear to be independent of the C-S-H composition. In ACW, within the uncertainty range of the measurements, similar R_d values were determined. The apparent positive effect on Np(IV) sorption in the presence of alkalis is considered to be not significant (compare Figures 5a with 5b and c). The constant R_d values observed for Np(IV) sorption, which is independent of the C-S-H composition, indicates that neither pH nor the Ca concentration have an influence on the uptake, suggesting that the $Np(OH)_4(aq)$ species sorbs onto the C-S-H phase as a fourfold hydrolyzed species like in the TiO_2 system. Note that recent EXAFS investigations provided clear evidence for the incorporation of Np(IV) in the interlayer of C-S-H phases independent of pH and C:S ratio [19]. This process is not controlled by a simple ion-exchange process, sub-

Brought to you by | Lib4RI Eawag-Empa
Authenticated
Download Date | 12/20/18 11:17 AM

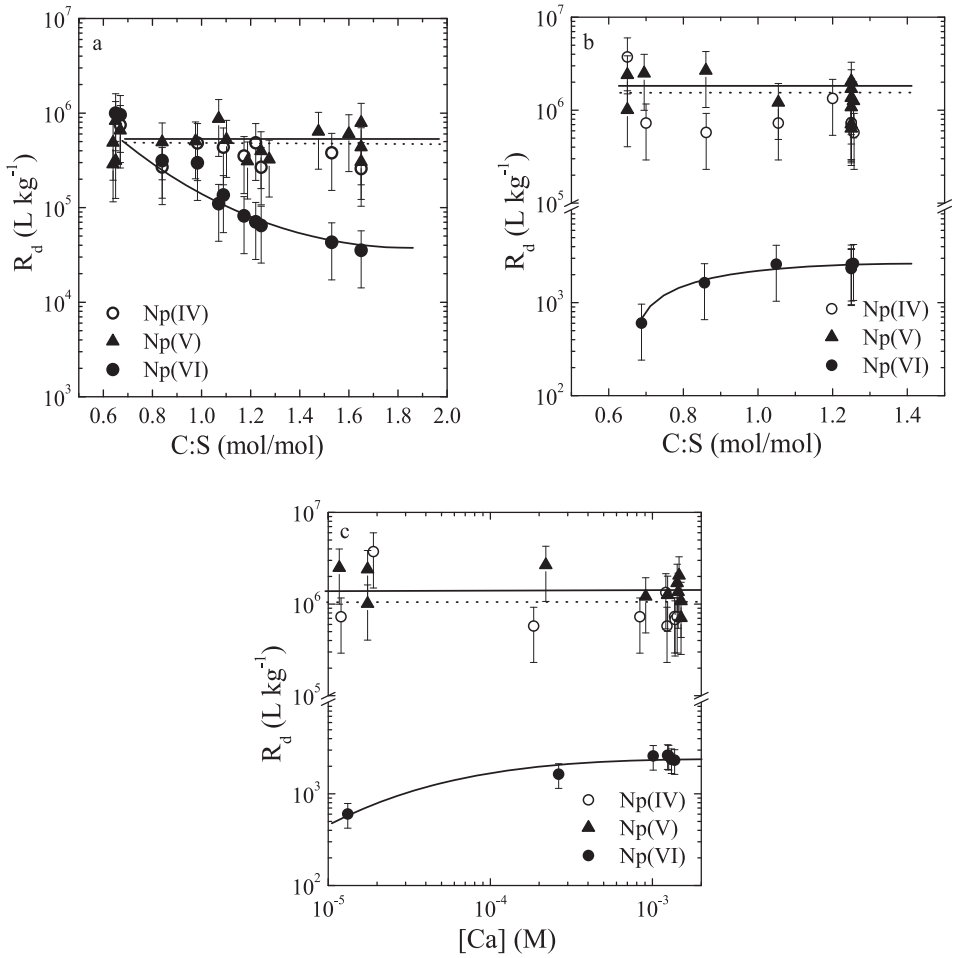

Fig. 5: Uptake of Np(IV,V,VI) by C-S-H phases. a) Effect of the C:S ratio under alkali-free conditions. b) Effect of C:S ratio in the presence of alkalis (ACW at pH = 13.3). c) Effect of the variation of the aqueous Ca concentration in the presence of alkalis (ACW at pH = 13.3). The Ca concentration range used as X axes in c) corresponds to equilibrium Ca concentrations with C-S-H phases at varying C:S ratios.

stituting a Np(IV) species for Ca in the interlayer, as a variation in the equilibrium Ca concentration over more than two orders of magnitude had no measurable effect on the R_d value (Figure 5c). This indicates that the Np(IV) species and Ca^{2+} occupy different crystallographic sites in the interlayer.

The uptake behaviour of Np(V) on C-S-H phases is very similar to that of Np(IV), *i.e.*, very high R_d values were observed independent of the C:S ratio. Identical R_d values for Np(IV) and Np(V) were also observed on TiO_2 at pH = 10. This sorption behaviour was unexpected as the lower effective charge of Np(V) (2.2) compared to Np(IV) (4.0) implies much weaker sorption of the pentavalent redox state compared to the tetravalent redox state.

Np(VI) exhibits a different sorption behaviour on C-S-H phases: In the absence of alkalis, R_d values at low C:S ratios are similar to those determined for Np(IV) and Np(V). With increasing C:S ratio, however, a steady decrease of the R_d values was observed.

In the case of Np(V) and Np(VI), a reversible adsorption process on C-S-H phases, similar to that on TiO_2 would imply that with increasing C:S ratio, the R_d values are affected simultaneously by two counteracting parameters: 1) a decrease in R_d value with increasing pH due to increasing concentrations of the non-sorbing anionic $Np^{V}O_2(OH)_2^-$ or $Np^{VI}O_2(OH)_4^{2-}$ complexes in solution, and 2) an increase in R_d value with increasing aqueous Ca concentration. Both effects may partially compensate each other, which complicates a direct comparison of the sorption behaviour on both solids. The sole effect of the aqueous Ca concentration on Np uptake by C-S-H phases is apparent from the sorption tests in the presence of alkalis (ACW, pH = 13.3) (Figures 5b, c). An increasing C:S ratio (*i.e.* increasing aqueous Ca concentration) appears to promote the sorption of anionic $Np^{VI}O_2(OH)_4^{2-}$

Brought to you by | Lib4RI Eawag-Empa
Authenticated
Download Date | 12/20/18 11:17 AM

hydrolysis species onto C-S-H phases. The R_d value for Np(VI) rises from 6×10^2 L kg^{-1} at a C:S ratio of 0.67 and a corresponding aqueous Ca concentration of 2×10^{-5} M to 2.5×10^3 L kg^{-1} at a C:S ratio of 1.25 and a corresponding aqueous Ca concentration of 1.6×10^{-3} M. This indicates that an increase in the aqueous Ca concentration of about two orders of magnitude gives rise to an increase in the R_d value by a factor 4. In the case of Np(V) no effect of an increase in the aqueous Ca concentration from 10^{-5} M to 10^{-3} M was observed (Figures 5b, c). Comparison of the Np sorption data on C-S-H phases (Figure 5c) with those on TiO_2 (Figure 4b) shows that the effect of the aqueous Ca concentration on the R_d values in the region 10^{-5} M < [Ca] < 10^{-3} M, is, at least qualitatively, rather similar in both cases. This suggests that the same processes might be involved.

4 Discussion

4.1 Effect of the Np redox state on sorption

At acidic pH, *i.e.* under conditions where the free metal cation dominates the speciation, R_d values for the sorption of pentavalent actinides on metal oxides and clays were found to be much lower than R_d values for the tetravalent and hexavalent actinides, for which hydrolysis is expected to take place already under very acidic conditions (*e.g.*, [62–64]). This sorption behaviour is generally understood as a result of the differences in effective charge of the respective redox states. At pH = 10, however, the present study shows that R_d values for Np(IV,V,VI) on TiO_2 and C-S-H phases are very similar in value. This unexpected sorption behaviour of the three Np redox states (*i.e.*, no effect of the effective charge) must originate from their different hydrolysis state at this pH.

A possible explanation might be found by considering the increasing electrostatic repulsion between the OH groups coordinated to actinide cations [65, 66] and the chemical similarity between hydrolysis reactions and complexation reactions with surface hydroxyl groups (*e.g.*, [51, 64, 67, 68]).

4.1.1 Electrostatic inter-ligand repulsion between coordinated OH groups

Neck and Kim [65, 66] showed that with increasing hydrolysis of an actinide, it becomes more difficult to add an additional OH group to its coordination sphere due to the increasing inter-ligand electrostatic repulsion. This results in a progressive decrease of the stepwise hydrolysis constants of an actinide with increasing number of OH groups in the coordination sphere. Stepwise hydrolysis reactions are usually written as:

$$M(OH)_{n-1}^{z-(n-1)} + H_2O \Leftrightarrow M(OH)_n^{z-n} + H^+ \qquad (3a)$$

The corresponding conditional stepwise hydrolysis constants ${}^*K'_n$ are defined by:

$${}^*K'_n = \frac{[M(OH)_n^{z-n}]\,[H^+]}{\left[M(OH)_{n-1}^{z-(n-1)}\right]} \qquad (3b)$$

"n" is an integer equal or greater than unity and "z" is the charge of the actinide cation.

In the approach of Neck and Kim [65, 66], the following basic relation occurs:

$$\log {}^*K'_n = \log {}^*K'_1 - \frac{{}^{rep}E_L}{RT \ln 10} \qquad (4)$$

With ${}^{rep}E_L$ being the electrostatic inter-ligand energy repulsion term and ${}^*K'_1$ the stability constant of the first hydrolyzed species, MOH^{z-1}.

Eq. (4) implies that the stepwise stability constant for the n^{th} hydrolysis species equals the stability constant of the first hydrolyzed species reduced with a term representing the electrostatic inter-ligand repulsion energy. Note that effects of electron-donating properties of coordinated OH groups to the effective charge of the hydrolysed Np species are not required in this approach which allows the decrease in stepwise hydrolysis constants to be quantified. The stability of a hydrolysed Np species is thus influenced by two factors: 1) the effective charge defining the bond strength between the hard Lewis acid (*e.g.* the free Np cation) and the hard base (*e.g.* the OH group), 2) the electrostatic inter-ligand repulsion. Inspection of the speciation of Np (Figure 1) reveals that, at pH = 10, the dominating species are $Np^{IV}(OH)_4$, $Np^{V}O_2^+$, $Np^{VI}O_2(OH)_3^-$. Based solely on the effective charge of the metal cations, the binding of an additional OH group to $Np^{V}O_2^+$ is expected to be much weaker (lower stepwise stability constant) at this pH than the binding of an additional OH group to $Np^{IV}(OH)_4$ and $Np^{VI}O_2(OH)_3^-$ (higher stepwise stability constants). However, a closer inspection of the thermodynamic databases reveals that the stepwise hydrolysis constants (at I = 0) for $Np^{V}O_2OH$ and $Np^{VI}O_2(OH)_4^{2-}$ are very similar (see Table 2): *i.e.*, $Np^{V}O_2OH$: $\log^* K_1^0 = -11.3$; $Np^{VI}O_2(OH)_4^{2-}$: $\log^* K_4^0 = -10.8$ [10]. This observation indicates that, despite the higher effective charge of Np(VI), the binding of an additional OH group to $Np^{V}O_2^+$ and $Np^{VI}O_2(OH)_3^-$ is equally strong at this pH. The electrostatic inter-ligand repulsion weakens the additional binding of a fourth OH group to $Np^{VI}O_2(OH)_3^-$ in such a way

Brought to you by | Lib4RI Eawag-Empa
Authenticated
Download Date | 12/20/18 11:17 AM

that its stepwise hydrolysis constant is equal in value to the stepwise hydrolysis constant of $Np^{V}O_2OH$. (Note that no thermodynamic data are available for the formation of the species $Np^{IV}(OH)_5^-$ and thus this species cannot be included in this comparison.)

4.1.2 Chemical similarity between hydrolysis reactions and complexation reactions with surface hydroxyl groups

The formation of a surface complex involves the replacement of a water molecule in the actinide coordination sphere by a surface OH group (Eq. 5a) in a way similar to that in hydrolysis reactions (Eq. 3a). (Note that H_2O molecules in the actinide coordination sphere are omitted in Eqs. (3a) and (5a).) Indeed, a stepwise surface complexation reaction can be written as follows

$$\equiv SOH + M(OH)_{n-1}^{z-(n-1)} \Leftrightarrow \equiv SO{-}M(OH)_{n-1}^{z-n} + H^+ \quad (5a)$$

with the corresponding conditional stepwise surface complexation constant, ${}^{S}K'_{n\text{-}1}$:

$${}^{S}K'_{n-1} = \frac{\left[\equiv SO{-}M(OH)_{n-1}^{z-n}\right]\left[H^+\right]}{\left[M(OH)_{n-1}^{z-(n-1)}\right]\left[\equiv SOH\right]} \quad (5b)$$

Thus, hydrolysis and surface complexation can be treated as related processes (*e.g.*, [51, 64, 67, 68]). It follows that the same factors; *i.e.*, the effective charge of the metal cation and the electrostatic inter-ligand repulsion, might affect the stepwise surface complexation constants of Np in the different redox states. Quantitatively, this means that values of the relevant stepwise surface complexation constants for actinides with different redox states will be similar at pH = 10, in the same way as their hydrolysis constants (see section 4.2.1.). In this context, similar R_d values for Np(IV), Np(V) and Np(VI) appear to be reasonable as a direct correlation exists between R_d values and stepwise surface complexation constants on the assumption that trace actinide concentrations are used ($[\equiv SOH] \approx ([\equiv SOH_{tot}] = \text{constant})$ and that chemical conditions (pH, aqueous composition, S/L) are constant. Under these conditions Eqs. (2) and (5b) can be combined as follows:

$$\frac{{}^{s}K'_{n-1}[\equiv SOH]}{[H^+]} = \text{constant} = R_d \times \left(\frac{m}{V}\right) \quad (6)$$

4.2 Effect of hydrolysis on the Np(IV,V,VI) sorption

The concept of electrostatic inter-ligand repulsion proposed by Neck *et al.* [65, 66] predicts a limiting hydrolysis number, n_{limit}, for each oxidation state of a given actinide. This is clearly demonstrated in Figure 1b in a paper published by Fanghänel *et al.* [69]: The figure shows that, in the case of the tetravalent actinides, measured values for the overall hydrolysis constant, $\log^{OH}\beta_n$, continue to increase up to $n = 4$. The concept predicts that the addition of a 5th OH ligand to the coordination sphere could still improve the stability of the complex suggesting a value for $n_{limit} > 4$. In the case of the hexavalent actinides, n_{limit} is predicted to be 4 as the addition of a 5th OH group would result in a decrease in the stability of the complex. In the case of the pentavalent actinides, Figure 1b in [69] indicates that n_{limit} is 2. Applied to the sorption data of the different redox states of Np, the concept implies that the formation of a surface complex adds an additional OH group to the coordination sphere of the metal center. Thus, the $Np^{IV}(OH)_4$ complex, which is still capable of accepting an additional oxygen-containing ligand in its coordination sphere ($n_{limit} > 4$), sorbs strongly on TiO_2 and C-S-H phases. In case of Np(VI), with $n_{limit} = 4$, the $Np^{VI}O_2(OH)_3^-$ complex is predicted to sorb, whereas the $Np^{VI}O_2(OH)_4^{2-}$ complex cannot extend its coordination sphere by an additional OH group, and therefore the species cannot form a surface bond. In the case of Np(V) with $n_{limit} = 2$, the $Np^{V}O_2OH$ complex can sorb, whereas the $Np^{V}O_2(OH)_2^-$ complex cannot form a surface bond. The above concept thus provides a qualitative understanding of the pH dependence of the Np(IV,V,VI) sorption on TiO_2.

To further assess whether or not the formation of non-sorbing $Np^{V}O_2(OH)_2^-$ and $Np^{VI}O_2(OH)_4^{2-}$ species can explain the reduction in R_d values for Np(V) and Np(VI) sorption on TiO_2, a reduction factor, F_{red}, was defined corresponding to the ratio of the R_d value in the absence (R_d^0) and in the presence (R_d) of the non-sorbing hydroxy species. In the following, the equation for F_{red} is deduced.

The stepwise hydrolysis reactions for Np(V) and Np(VI) can be written in the following general form:

$$NpO_2(OH)_{n-1}^{z-4-(n-1)} + H_2O \Leftrightarrow NpO_2(OH)_n^{z-4-n} + H^+ \quad (7a)$$

with the corresponding conditional stepwise hydrolysis constant, ${}^{*}K'_n$:

$${}^{*}K'_n = \frac{\left[NpO_2(OH)_n^{z-4-n}\right]\left[H^+\right]}{\left[NpO_2(OH)_{n-1}^{z-4-(n-1)}\right]} \quad (7b)$$

Brought to you by | Lib4RI Eawag-Empa
Authenticated
Download Date | 12/20/18 11:17 AM

Eqs. (7a) and (7b) correspond to Eqs. (3a) and (3b) with "M" = NpO_2^{z-4}, "z" is either +5 or +6 depending on the Np redox state and "n" = 2 (Np(V)) or 4 (Np(VI)).

Above pH = 10, the definition of R_d in Eq. (2) can be rewritten as:

$$R_d = \frac{\{NpO_2^{z-4}\}_{sorb}}{\left(\left[NpO_2(OH)_{n-1}^{z-4-(n-1)}\right] + \left[NpO_2(OH)_n^{z-4-n}\right]\right)} \quad (8)$$

Combining Eqs. (7b) and (8) gives:

$$R_d = \frac{\{NpO_2^{z-4}\}_{sorb}}{\left(\left[NpO_2(OH)_{n-1}^{z-4-(n-1)}\right] \cdot \left(1 + {}^*K'_n / [H^+]\right)\right)} \quad (9)$$

Assuming linear sorption, $\frac{\{NpO_2^{z-4}\}_{sorb}}{\left[NpO_2(OH)_{n-1}^{z-4-(n-1)}\right]} = R_d^0$, Eq. (9) can be written as:

$$R_d = \frac{R_d^0}{\left(1 + \frac{{}^*K'_n}{[H^+]}\right)} \quad (10)$$

Eq. (10) can then be reorganized to give the following definition of F_{red}:

$$F_{red} = \frac{R_d^0}{R_d} = 1 + \frac{{}^*K'_n}{[H^+]} \quad (11)$$

F_{red} is valid for all solids provided the hydrolysed species $NpO_2(OH)_n^{z-4-n}$ does not sorb, the sorption of the species $NpO_2(OH)_{n-1}^{z-4-(n-1)}$ is linear and reversible and the sorbent remains stable throughout the sorption experiment. The non-sorbing species are $Np^VO_2(OH)_2^-$ and $Np^{VI}O_2(OH)_4^{2-}$. The R_d values in the pH range 10 < pH<14 can then be calculated as $R_d = R_d^0/F_{red}$.

It was assumed that the R_d values determined at pH = 10 correspond to R_d^0. $\log^* K_n^0$ values at I = 0 are listed in Table 2. Ionic strength corrections for the calculation of the conditional stability constants, $\log^* K'_n$, were carried out using the SIT approach and ion interaction coefficients (ε) taken from [9]: ($\varepsilon(H^+,Cl^-) = 0.12 \pm 0.01$ kg mol^{-1}, $\varepsilon(Na^+,NpO_2(OH)_2^-) = -0.01 \pm 0.07$ kg mol^{-1}), and from [10]: $\varepsilon(Na^+,NpO_2(OH)_3^-) = -0.20$ kg mol^{-1}, $\varepsilon(Na^+,NpO_2(OH)_4^{2-}) = -0.12$ kg mol^{-1}). For $\varepsilon(H^+,OH^-)$, the same value as for $\varepsilon(H^+,Cl^-)$ was selected. The pH dependence of the R_d values for Np(V) and Np(VI) sorption on TiO_2 could successfully be described with this model (Figure 6). This finding supports the idea that $Np^VO_2(OH)_2^-$ and $Np^{VI}O_2(OH)_4^{2-}$ species are limiting hydroxy complexes which cannot form surface bonds on TiO_2.

Table 2: Overall ($\log^* \beta_n^0$) and stepwise ($\log^* K_n^0$) formation constants for relevant Np(V) and Np(VI) hydrolysis complexes used in the model calculations.

$NpO_2^{z-4} + nH_2O \Longleftrightarrow NpO_2(OH)_n^{z-4-n} + nH^+ \qquad \log^* \beta_n^0$

$NpO_2(OH)_{n-1}^{z-4-(n-1)} + H_2O \Leftrightarrow NpO_2(OH)_n^{z-4-n} + H^+ \qquad \log^* K^0$

	$\log^* \beta_n^0$	$\log^* K_n^0$
$Np^VO_2OH(aq)$	−11.3[a]	−11.3
$Np^VO_2(OH)_2^-$	−23.6[a]	−12.3
$Np^{VI}O_2(OH)^+$	−5.1[a]	−5.1
$Np^{VI}O_2(OH)_2(aq)$	−12.21[b]	−7.11
$Np^{VI}O_2(OH)_3^-$	−21.2[c]	−8.99
$Np^{VI}O_2(OH)_4^{2-}$	−32.0[c]	−10.8

[a] Guillaumont *et al.* [9];
[b] Estimated by correlation with Z_{eff} [5];
[c] Gaona *et al.* [10].

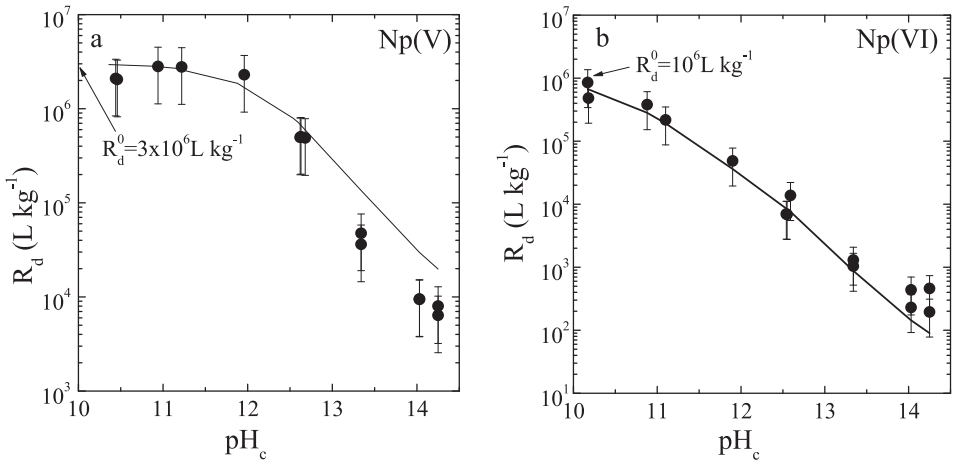

Fig. 6: pH dependence of the sorption of Np(V) (a) and Np(VI) (b) on TiO_2. Experimental data (symbols) and modeling (lines) (see text).

Brought to you by | Lib4RI Eawag-Empa
Authenticated
Download Date | 12/20/18 11:17 AM

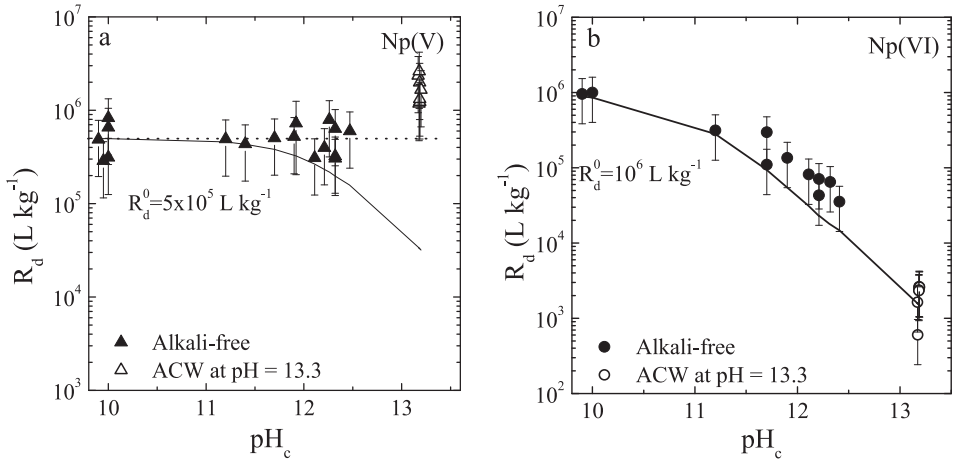

Fig. 7: pH dependence of the sorption of Np(V) (a) and Np(VI) (b) on C-S-H phases under alkali-free conditions and in the presence of alkalis (ACW; pH = 13.3). Experimental data (symbols) and modeling (lines) (see text).

4.3 Implications for Np(IV,V,VI) sorption on C-S-H phases

In Figures 7a and 7b, the same concept has been applied to model the sorption data of Np(V) and Np(VI) on C-S-H phases with different C:S ratios. Note that the well-known changes in C-S-H structures with varying pH and various aqueous Ca concentrations (*e.g.*, [31, 32]) are not taken into account. This model only quantifies the contribution of the aqueous Np(IV,V,VI) speciation to their sorption behaviour on C-S-H phases assuming that the aqueous speciation has the same influence on the sorption on C-S-H phases and on TiO_2; *i.e.* strong sorption of $Np^{IV}(OH)_4(aq)$, $Np^{V}O_2OH(aq)$, $Np^{VI}O_2(OH)_3^-$ and no sorption of $Np^{V}O_2(OH)_2^-$ and $Np^{VI}O_2(OH)_4^{2-}$.

The figures show that in the case of Np(VI), the proposed model approach enables us to explain the pH dependence of the experimental data. The effect of the C:S ratio on the sorption of Np(VI) by C-S-H phases can be attributed to the formation of the non-sorbing $NpO_2(OH)_4^{2-}$ complex. There could be a small effect of the Ca concentration on sorption as shown in Figures 5a, b, but this effect appears to be negligible compared to the hydrolysis effect. In the case of Np(V), the proposed approach allows the sorption data on C-S-H phases in the absence of alkalis to be modeled up to a pH of 12.5. The high R_d values in the presence of alkalis (in ACW) at pH = 13.3 are however not explained by the model (Figure 7a). Furthermore, Figure 5c shows that these high R_d values are independent of the Ca concentration. Hence, the high R_d values observed for Np(V) sorbed on C-S-H phases at pH = 13.3 result from an additional stabilization of the local coordination environment of the sorbed Np(V) species.

It should be noted that the present macroscopic observations are not necessarily incompatible with the previous EXAFS studies which indicated Np(IV,V,VI) incorporation into the C-S-H interlayers [19, 22, 24, 27, 28]. The electrostatic ligand repulsion in the coordination sphere of the actinides is also expected to be effective in case of actinide sorption *via* the formation of an inner-sphere complex in the C-S-H interlayers.

5 Conclusions

Sorption studies with Np(IV,V,VI) on TiO_2 and C-S-H phases under alkaline conditions reveal strong sorption and the same R_d values for all three redox states at pH ~ 10. Increasing pH values give rise to a significant decrease of the R_d values for Np(V) and Np(VI) sorption on TiO_2 whereas increasing aqueous Ca concentrations give rise to higher R_d values for the two redox states. An influence of pH and aqueous Ca concentration on the R_d value of Np(IV) was not observed. The identical, high R_d values at pH ~ 10 and the effect of pH on sorption is interpreted in terms of an increasing inter-ligand electrostatic repulsion in the Np coordination sphere with progressing hydrolysis. A mechanistic explanation for the observed effect of Ca on Np(V,VI) sorption is still lacking.

Based on the wet chemistry data determined in the present work, the sorption behaviour Np(IV) and Np(VI) onto C-S-H phases can be described almost entirely by invoking a predominant effect of hydrolysis as in the case of sorption onto TiO_2. The high R_d values for Np(V) uptake by C-S-H phases in ACW (pH = 13.3), however, are inconsistent with the formation of a non-sorbing $Np^{V}O_2(OH)_2^-$

Brought to you by | Lib4RI Eawag-Empa
Authenticated
Download Date | 12/20/18 11:17 AM

complex. Uptake of the latter complex by C-S-H phases can only be explained on the assumption that additional energetic stabilization occurs in the coordination environment of this Np(V) species, which is presumably taken up into the C-S-H interlayer.

Acknowledgement: The research leading to these results has received funding from the European Union's European Atomic Energy Community's (Euratom) Seventh Framework Programme FP7/2007-2011 under grant agreement no. 212287 (RECOSY project). Partial financial support was provided by the National Cooperative for the Disposal of Radioactive Waste (Nagra), Switzerland. X.G. acknowledges the Generalitat de Catalunya for his post-doctoral grant ("Beatriu de Pinós" program).

Received June 5, 2013; accepted August 27, 2013.

References

1. Miller, W., Alexander, R., Chapman, N., Mckinley, I., Smellie, J.: Geological Disposal of radioactive wastes and natural analogues. Lessons from nature and archeology. Elsevier/Pergamon: Amsterdam, The Netherlands, 2000.
2. Evans, N. D. M.: Binding mechanisms of radionuclides to cement. Cem. Concr. Res. **38**, 543–553 (2008).
3. Mandaliev, P., Wieland, E., Dähn, R., Tits, J., Churakov, S. V., Zaharko, O.: Mechanisms of Nd(III) uptake by 11Å tobermorite and xonotlite. Appl. Geochem. **25**, 763–777 (2010).
4. Schmidt, J., Vogelsberger, W.: Aqueous long-term solubility of titania nanoparticles and titanium(IV) hydrolysis in a sodium chloride system studied by adsorptive stripping voltammetry. J. Solution Chem. **38**, 1267–1282 (2009).
5. Gaona, X., Tits, J., Dardenne, K., Liu, X., Rothe, J., Denecke, M. A., Wieland, E., Altmaier, M.: Spectroscopic investigations of Np(V/VI) redox speciation in hyperalkaline TMA–OH solutions. Radiochim. Acta **100**, 759–770 (2012).
6. Wieland, E., Van Loon, L. R.: Cementitious near-field sorption database for performance assessment of an ILW repository in Opalinus Clay. PSI Bericht 03-06, Paul Scherrer Institut, Villigen, Switzerland and Nagra Technical Report NTB 02-20, Nagra, Wettingen, Switzerland, 2003.
7. Choppin, G. R.: Solution chemistry of actinides. Radiochim. Acta **32**, 43–53 (1983).
8. Choppin, G. R.: Complexation of pentavalent and hexavalent actinides by fluoride. Radiochim. Acta **37**, 143–146 (1984).
9. Guillaumont, R., Fanghänel, T., Fuger, J., Grenthe, I., Neck, V., Palmer, D. A., Rand, M. H.: Chemical Thermodynamics Vol. 5. Update on the Chemical Thermodynamics of Uranium, Neptunium, Plutonium, Americium and Technetium. Elsevier, North Holland: Amsterdam, The Netherlands, Vol. 5, 2003.
10. Gaona, X., Fellhauer, D., Altmaier, M.: Thermodynamic description of Np(VI) solubility, hydrolysis and redox behaviour in dilute to concentrated alkaline NaCl solutions. Pure Appl. Chem. **85**, 2027–2049 (2013).
11. Berner, U.: Project Opalinus Clay: Radionuclide concentration limits in the cementitious near-field of an ILW repository. PSI Bericht Nr. 02-26, Paul Scherrer institut, Villigen, Switzerland and Nagra Technical Report NTB 02-22, Wettingen, Switzerland, 2003.
12. Wersin, P., Johnson, L. H., Schwyn, B., Berner, U., Curti, E.: Redox Conditions in the Near Field of a Repository for SF/HLW and ILW in Opalinus Clay. Nagra Technical Report NTB 02-13, Wettingen, Switzerland, 2003.
13. Allard, B.: Radionuclide sorption in concrete. Nagra Technical Report, NTB 85-21, Nagra, Wettingen, Switzerland, 1985.
14. Höglund, S., Eliason, L., Allard, B., Andersonn, K., Torstenfeld, B.: Sorption of some fission products and actinides in concrete systems. Mat. Res. Soc. Symp. Proc. **807**, 683–690 (1985).
15. Holgersson, S., Albinsson, Y., Allard, B., Boren, H., Pavasars, I., Engkvist, I.: Effects of gluco-isosaccharinate on Cs, Ni, Pm, and Th sorption onto, and diffusion into cement. Radiochim. Acta **82**, 393 - 398 (1998).
16. Tits, J., Wieland, E., Bradbury, M. H., Dobler, J.-P.: The uptake of Eu(III) and Th(IV) by cement-type minerals in the alkaline disturbed zone of a nuclear waste repository. Balkema: Rotterdam, The Netherlands, 2000, p 691 - 694.
17. Wieland, E., Tits, J., Spieler, P., Dobler, J. P.: Interaction of Eu(III) and Th(IV) with sulphate-resisting Portland cement. Mat. Res. Soc. Symp., 1998, Vol. 506, pp 573–578.
18. Wieland, E., Tits, J., Dobler, J.-P., and Spieler, P.: The effect of a-isosaccharinic acid on the stability of, and Th(IV) uptake by hardened cement paste. Radiochim. Acta **90**, 683 - 688 (2002).
19. Gaona, X., Dähn, R., Tits, J., Scheinost, A., Wieland, E.: Uptake of Np(IV) by C-S-H phases and cement paste: an EXAFS study. Environ. Sci.Technol. **45**, 8765–8771 (2011).
20. Wang, L., Martens, E., Jacques, D., De Canniere, P., Berry, J., Mallants, D.: Review of sorption values for the cementitious near-field of a near surface radioactive disposal facility. NIROND-TR report 2008-23 E, ONDRAF / NIRAS, Brussels, Belgium 2009.
21. Sylwester, E. R., Allen, P. G., Zhao, P., Viani, B. E.: Interactions of uranium and neptunium with cementitious materials studied by XAFS. Mat. Res. Soc. Symp. Proc. **608**, 307 - 312 (2000).
22. Gaona, X., Wieland, E., Tits, J., Scheinost, A., Dähn, R.: Np(V/VI) redox chemistry in cementitious systems: XAFS investigations on the speciation under anoxic and oxidizing conditions. Appl. Geochem. **28**, 109–118 (2013).
23. Pointeau, I., Landesman, C., Giffault, E., Reiller, P.: Reproducibility of the uptake of U(VI) onto degraded cement pastes and calcium silicate hydrate phases. Radiochim. Acta **92**, 645 - 650 (2004).
24. Harfouche, M., Wieland, E., Dähn, R., Fujita, T., Tits, J., Kunz, D., Tsukamoto, M.: EXAFS study of U(VI) uptake by calcium silicate hydrates. J. Colloid Interface Sci. **303**, 195–204 (2006).

Brought to you by | Lib4RI Eawag-Empa
Authenticated
Download Date | 12/20/18 11:17 AM

25. Pointeau, I., Coreau, N., Reiller, P. E.: Uptake of anionic radionuclides onto degraded cement pastes and competing effect of organic ligands. Radiochim. Acta **96**, 367–374 (2008).
26. Tits, J., Fujita, T., Tsukamoto, M., Wieland, E.: Uranium(VI) uptake by synthetic calcium silicate hydrates. Mat. Res. Soc. Symp. Proc. **1107**, 467–474 (2008).
27. Tits, J., Geipel, G., Macé, N., Eilzer, M., Wieland, E.: Determination of uranium(VI) sorbed species in calcium silicate hydrate phases. A laser-induced luminescence spectroscopy and batch sorption study. J. Colloid Interface Sci. **359**, 248–256 (2011).
28. Macé, N., Wieland, E., Dähn, R., Tits, J., Scheinost, A.: EXAFS investigation on U(VI) immobilization in hardened cement paste: Influence of experimental conditions on speciation. Radiochim. Acta **101**, 379–389 (2013).
29. Gaona, X., Kulik, D., Macé, N., Wieland, E.: Aqueous–solid solution thermodynamic model of U(VI) uptake in C-S-H phases. Appl. Geochem. **27**, 81–95 (2012).
30. Chen, J. J., Thomas, J. J., Taylor, H. F. W., Jennings, H. M.: Solubility and structure of calcium silicate hydrates. Cem. Concr. Res. **34**, 1499–1519 (2004).
31. Richardson, I. G.: The calcium silicate hydrates. Cem. Concr. Res. **38**, 137–158 (2008).
32. Garbev, K., Beuchle, G., Bornefeld, M., Black, L., Stemmermann, P.: Cell Dimensions and composition of nanocrystalline calcium silicate hydrate solid solutions. Part 1: Synchrotron-based X-ray diffraction. J. Am. Ceram. Soc. **91**(9), 3005–3014 (2008).
33. Berner, U. R.: Modelling the incongruent dissolution of hydrated cement minerals. Radiochim. Acta **44/45**, 387–393 (1988).
34. Berner, U. R.: Evolution of pore water chemistry during degradation of cement in a radioactive waste repository environment. Waste Manage. **12**, 201–219 (1992).
35. Kulik, D. A.: Improving the structural consistency of C-S-H solid solution thermodynamic models. Cem. Concr. Res. **41**, 477–495 (2011).
36. Comarmond, M. J., Payne, T. E., Harrison, J. J., Thiruvoth, S., Wong, H., Augterson, R. D., Lumpkin, G. R., Müller, K., Foerstendorf, H.: Uranium sorption on various forms of titanium dioxide - influence of surface area, surface charge, and impurities. Environ. Sci. Technol. **45**, 5536–5542 (2011).
37. Atkins, M., Glasser, F. P., Kindness, A.: Cement hydrate phases: Solubility at 25° C. Cem. Concr. Res. **22**, 241–246 (1992).
38. Tits, J., Wieland, E., Müller, C. J., Landesman, C., Bradbury, M. H.: Strontium binding by calcium silicate hydrates. J. Colloid Interface Sci. **300**, 78–87 (2006).
39. Sill, C. W.: Preparation of Neptunium-239 tracer. Anal. Chem. **38**(6), 802–804 (1966).
40. Altmaier, M., Metz, V., Neck, V., Müller, R., Fanghänel, T.: Solid-liquid equilibria of $Mg(OH)_2$(cr) and $Mg_2(OH)_3Cl_4H_2O$(cr) in the system Mg–Na–H–OH–O–Cl–H_2O at 25° C. Geochim. Cosmochim. Acta **67**, 3595–3601 (2003).
41. Rojo, H., Tits, J., Gaona, X., Garcia-Gutierrez, M. G., Missana, T., Wieland, E.: Thermodynamics of Np(IV) complexes with gluconic acid under alkaline conditions: sorption studies. Radiochim. Acta **101**, 133–138 (2013).
42. Tits, J., Bradbury, M. H., Eckert, P., Schaible, A.: The uptake of Eu and Th by calcite under high pH cement pore water conditions. PSI Bericht Nr. 02-03, Paul Scherrer Institut, Villigen, Switzerland and Nagra Technical Report NTB 02-08, Nagra, Wettingen, Switzerland, 2002.
43. Guo, Z., Yan, Z., Tao, Z.: Sorption of uranyl ions on TiO_2: Effects of contact time, ionic strength, concentration and humic substance. J. Radioanal. Nucl. Chem. **261**(1), 157–162 (2004).
44. Guo, Z., Niu, L., Tao, Z.: Sorption of Th(IV) ions onto TiO_2: Effects of contact time, ionic strength, thorium concentration and phosphate. J. Radioanal. Nucl. Chem. **266**(2), 333–338 (2005).
45. Bertetti, F. P., Pabalan, R. T., Almendarez, M. G.: Studies of Neptunium(V) sorption on quartz, clinoptilolite, montmorillonite, and α-alumina. in: Adsorption of metals by geomedia, Academic press: San Diego, CA., USA, 1998, pp 131–148.
46. Pathak, P. N., Choppin, G. R.: Sorption of neptunyl(V) cations on suspended silicate: Effects of pH, ionic strength, complexing anions, humic acid, and metal ions. J. Radioanal. Nucl. Chem. **274**(1), 53–60 (2007).
47. Amayri, S., Jermolayev, A., Reich, T.: Neptunium(V) sorption on kaolinite. Radiochim. Acta **99**, 349–357 (2011).
48. Tinnacher, R. M., Zavarin, M., Powell, B. A., Kersting, A. B.: Kinetics of neptunium(V) sorption and desorption on goethite: An experimental and modeling study. Geochim. Cosmochim. Acta **75**, 6584–6599 (2011).
49. Hsi, C.-K. D., Langmuir, D.: Adsorption of uranyl onto ferric oxyhydroxides: Application of the surface complexation site-binding model. Geochim. Cosmochim. Acta **49**, 1931–1941 (1985).
50. Jakobsson, A.-M.: Measurement and modeling of Th sorption onto TiO_2. J. Colloid Interface. Sci. **220**, 367–373 (1999).
51. Bradbury, M. H., Baeyens, B.: Sorption modelling on illite. Part II: Actinide sorption and linear free energy relationships. Geochim. Cosmochim. Acta **73**, 1004–1013 (2009).
52. Kohler, M., Honeyman, B. D., Leckie, J. O.: Neptunium(V) sorption on hematite (α-Fe_2O_3) in aqueous suspension: The effect of CO_2. Radiochim. Acta **85**, 33–48 (1999).
53. Gorgeon, L.: Contribution à la modélisation physico-chimique de la rétention de radioéléments à vie longue par des matériaux argileux. PhD thesis, Université Paris 6, Paris France, 1994.
54. Turner, D. R., Pabalan, R. T., Bertetti, F. P.: Neptunium(V) sorption on montmorillonite: an experimental and surface complexation modeling study. Clays Clay Miner. **46**(3), 256–269 (1998).
55. Khasanova, A. B., Kalmykov, S. N., Perminova, I. V., Clark, S. B.: Neptunium redox behavior and sorption onto goethite and hematite in the presence of humic acids with different hydroquinone content. J. Alloys Comp. **444–445**, 491–494 (2007).
56. Yates, D. E., James, R. O., Healy, T. E.: Titanium dioxide–electrolyte interface. Part 1. Gas adsorption and tritium exchange studies, J. Chem. Soc. Faraday Trans. I. **76**, 1–8 (1980).
57. Davis, J., Kent, D. B.: Surface complexation modelling in aqueous geochemistry. In: *Mineral-Water Interface Geochemistry* (Hochella, M. F., White, A. F. eds.) Vol. 23, Mineralogical Society of America: Washington, DC, 1990, p 177–260.
58. Jang, H. M., Fürstenau, D. W.: The specific adsorption of alkaline-earth cations at the rutile/water interface. Coll. Surf. **21**, 235–257 (1986).
59. Ridley, M. K., Machesky, M. L., Wesolowski, D. J., Palmer, D. A.: Calcium adsorption at the rutile-water interface: A potentiometric study in NaCl media to 250° C. Geochim. Cosmochim. Acta **63**, 3087–3096 (1999).
60. Ridley, M. K., Machesky, M. L., Wesolowski, D. J., Palmer, D. A.: Modeling the surface complexation of calcium at the rutile-

Brought to you by | Lib4RI Eawag-Empa
Authenticated
Download Date | 12/20/18 11:17 AM

water interface to 250° C. Geochim. Cosmochim. Acta **68**(2), 239–251 (2004).
61. Ridley, M. K., Hiemstra, T., Van Riemsdijk, W. H., Machesky, M. L.: Inner-sphere complexation of cations at the rutile–water interface: A concise surface structural interpretation with the CD and MUSIC model. Geochim. Cosmochim. Acta **73**, 1841–1856 (2009).
62. Lieser, K. H., Thybusch, B.: Sorption of uranyl ions on titanium dioxide. Fresenius, Z. Anal. Chem. **332**, 351–357 (1988).
63. Choppin, G. R.: Actinide speciation in aquatic systems. Marine Chem. **99**(1–4), 83–92 (2006).
64. Bradbury, M. H., Baeyens, B.: Modelling the sorption of Mn(II), Co(II), Ni(II), Zn(II), Cd(II), Eu(III), Am(III), Sn(IV), Th(IV), Np(V) and U(VI) on montmorillonite: Linear free energy relationships and estimates of surface binding constants for some selected heavy metals and actinides. Geochim. Cosmochim. Acta **69**, 875–892 (2005).
65. Neck, V., Kim, J. I.: An electrostatic approach for the prediction of actinide complexation constants with inorganic ligands – application to carbonate complexes. Radiochim. Acta **88**, 815–822 (2000).
66. Neck, V., Kim, J. I.: Solubility and hydrolysis of tetravalent actinides. Radiochim. Acta **89**, 1–16 (2001).
67. Schindler, P. W., Wälti, E., Fürst, B.: The role of surface hydroxyl groups in the surface chemistry of metal oxides. Chimia **30**(2), 107–109 (1976).
68. Dzombak, D. A., Morel, F. M.: Surface Complexation Modeling. 1 ed., John Wiley and Sons, New-York 1990, p 393.
69. Fanghänel, T., Neck, V.: Aquatic chemistry and solubility phenomena of actinide oxides / hydroxides. Pure Appl. Chem. **74**(10), 1895–1907 (2002].

Brought to you by | Lib4RI Eawag-Empa
Authenticated
Download Date | 12/20/18 11:17 AM